



## Short communication

Calcium doped  $Y_3Fe_5O_{12}$  as a new cathode material for intermediate temperature solid oxide fuel cellsWei Zhong<sup>a</sup>, Yihan Ling<sup>a</sup>, Yuanyuan Rao<sup>a</sup>, Ranran Peng<sup>a,\*</sup>, Yalin Lu<sup>a,b,\*\*</sup><sup>a</sup>CAS Key Laboratory of Materials for Energy Conversion, Department of Materials Science and Engineering, University of Science and Technology of China, Jinzhai Road 96, Hefei 230026, PR China<sup>b</sup>Hefei National Laboratory for Physical Sciences at Microscale, University of Science and Technology of China, Hefei 230026, PR China

## ARTICLE INFO

## Article history:

Received 19 January 2012

Received in revised form

13 March 2012

Accepted 15 March 2012

Available online 21 April 2012

## Keywords:

Solid oxide fuel cells

Cathode

Triple-phase boundaries

Rate-limiting steps

Garnet

## ABSTRACT

Calcium doped yttrium iron garnet,  $Y_{2.5}Ca_{0.5}Fe_5O_{12-\delta}$  (YCFO), was studied as a new cathode material for intermediate temperature solid oxide fuel cells. Low polarization resistance of  $0.55 \Omega\text{cm}^2$  at  $650^\circ\text{C}$  was realized with the use of YCFO– $Ce_{0.8}Sm_{0.2}O_{1.9}$  (SDC, 40 wt.%) composite electrode. An investigation over limiting steps of the cathode reaction suggests that oxygen ion diffusion, oxygen dissociative adsorption, and gas-phase diffusion might be the rate-limiting steps for the YCFO–SDC cathode. Of a single cell using the YCFO–SDC composite cathode, the polarization resistance reduces to as low as  $0.14 \Omega\text{cm}^2$  measured at  $650^\circ\text{C}$ , and the maximum power density reaches  $438 \text{ mW cm}^{-2}$  with a  $40 \mu\text{m}$  – thick SDC electrolyte.

© 2012 Elsevier B.V. All rights reserved.

## 1. Introduction

Finding suitable cathode materials is crucial to intermediate temperature solid oxide fuel cells (IT-SOFCs) with the goal to improve their catalytic activity at the reduced operating temperatures. To meet the reaction demand on both electronic and ionic conducting paths, an effective cathode material for IT-SOFCs has been mainly reported as the electronic–ionic mixed conductors, which includes the doped perovskite [1–14], double perovskite oxides [15–18], and  $K_2NiF_4$  type oxides [19,20]. Among such mixed conductors, cobalt-based perovskite or ordered–double perovskite oxides, such as  $La_{0.8}Sr_{0.2}CoO_{3-\delta}$  (LSC) [1],  $La_{0.6}Sr_{0.4}Co_{0.2}Fe_{0.8}O_{3-\delta}$  (LSCF) [2–6],  $Sm_{0.5}Sr_{0.5}CoO_{3-\delta}$  (SSC) [7–11], and  $Ba_{0.5}Sr_{0.5}Co_{0.8}Fe_{0.2}O_{3-\delta}$  (BSCF) [11–14], have been found to exhibit fairly good electrochemical activity to oxygen reduction. For example, low interfacial polarization resistances of 0.33, 0.18 and  $0.064 \Omega\text{cm}^2$  at  $600^\circ\text{C}$  were achieved in LSCF– $Ce_{0.8}Gd_{0.2}O_3$  (GDC) [2], SSC– $Ce_{0.8}Sm_{0.2}O_{1.9}$  (SDC) [7] and BSCF–SDC composite cathodes

[12], respectively. In such composite cathodes, doped ceria was normally added in order to enlarge the length of triple-phase boundaries (TPBs). However, the high contents of non-earth-abundant lanthanide and cobalt elements in these materials had led to a high cost of the resulting cells [21]. Therefore, a new electrochemical active cathode using as much as possible earth-abundant materials would be important for commercializing such IT-SOFCs at the market-acceptable prices.

Yttrium iron garnet,  $Y_3Fe_5O_{12}$  (YIG), had drawn much attention in the past as a promising ferrimagnetic oxide, and was widely applied in microwave and magneto-optic devices [22]. With the introduction of lower valence cations, such as  $Ca^{2+}$ , into A-site, relatively high specific oxygen permeability with the value of  $10^{-11} \text{ mol s}^{-1} \text{ cm}^{-2}$  could be achieved [23]. In addition, the thermal expansion coefficient (TEC) of YIG was approximately  $10.6 \times 10^{-6} \text{ K}^{-1}$  [23], which was very close to those of stabilized zirconia ( $10.5 \times 10^{-6} \text{ K}^{-1}$  [24]) and doped ceria ( $11.4 \times 10^{-6} \text{ K}^{-1}$  [25]) electrolytes. It should be reasonable to predict the potential use of the modified garnet as a cathode material in SOFCs. Unfortunately, little investigation has been put on utilizing a garnet as cathodes in the past, except that it was referred as an undesirable product from the reaction between electrolyte and cathode in one literature [26]. In this research, we thoroughly investigated the use of garnet  $Y_{2.5}Ca_{0.5}Fe_5O_{12}$  (YCFO) as a cathode material for IT-SOFCs. Polarization resistances of the

\* Corresponding author. Tel./fax: +86 551 3600594.

\*\* Corresponding author. Hefei National Laboratory for Physical Sciences at Microscale, University of Science and Technology of China, Hefei 230026, PR China. Tel./fax: +86 551 3603004.

E-mail addresses: pengrr@ustc.edu.cn (R. Peng), yllu@ustc.edu.cn (Y. Lu).

YCFO–SDC composite cathodes were studied as functions of the weight ratio of the SDC phase, the tested temperature, and the oxygen partial pressure using symmetric cells. Electrochemical performances of single cells using the YCFO-based composite cathodes were also characterized in details.

## 2. Experimental

### 2.1. Preparation of powders, symmetric cells and single cells

The powders involved in this study, including  $Y_{2.5}Ca_{0.5}Fe_5O_{12-\delta}$  (YCFO),  $Ce_{0.8}Sm_{0.2}O_{1.9}$  (SDC) [27] and NiO [28], were all synthesized by the glycine nitrate process. The detailed synthesis procedure for YCFO powders was shown as follows. Proper amount of  $Y_2O_3$  powders were dissolved in dilute nitrate to form an yttrium nitrate solution. Stoichiometric amount of  $Ca(NO_3)_2 \cdot 4H_2O$  and  $Fe(NO_3)_3 \cdot 9H_2O$  were dissolved in distilled water, and then mixed with the yttrium nitrate solution. Glycine, working both as a combination agent and as a fuel, was added into the nitrate solution with the glycine/nitrate molar ratio of 0.5:1. The formed solution was heated on an electric oven till self-combustion occurred. The as-synthesized powders were subsequently fired at 1100 °C for 2 h to obtain YCFO powders. YCFO–SDC composite powders with the weight ratio of 1:1 were fired at 1100 °C for 2 h to evaluate their chemical compatibility.

To make electrical conductivity measurement, YCFO powders were shaped into a rectangular bar by cold-pressing technique, and then sintered at 1350 °C for 5 h in air. The sintered bar was approximately 36.52 mm in length, 6.12 mm in width, and 2.05 mm in height. Four silver wires were wound tightly around the sintered samples as current collector, in which the two outer electrodes 32.30 mm apart supplied the current and the two inner electrodes 23.06 mm apart measured the potential drop.

Symmetric cells were fabricated with SDC as electrolytes. SDC powders were cold-pressed at 220 MPa into disks about 13 mm in diameter and 1 mm in thickness, and then sintered at 1400 °C for 5 h in air as electrolyte substrates. YCFO and SDC powders were mixed at an SDC weight ratio ranging from 0 to 60% as composite electrodes. Screen-printing technique was applied to fabricate the YCFO–SDC composite electrode film on both surfaces of the SDC disks with 6 wt.% ethylcellulose–terpineol as organic binder. The samples were then fired at 1100 °C for 2 h to complete the fabrication procedure. YCFO–SDC composite cathodes were abbreviated as YCFO–SDC $x$ , where the number  $x$  after SDC denoted the weight percentage of SDC in the composites. For example, YCFO–SDC40 meant 40 wt.% SDC in the composite cathode.

Single cells were fabricated by a co-pressing technique. NiO and SDC powders were mixed at the weight ratio of 65:35 as a composite anode. Bi-layers of the anode substrate and SDC electrolyte were co-pressed at 250 MPa and then sintered at 1250 °C for 5 h to obtain a dense SDC membrane. YCFO–SDC40 composite cathodes were prepared by the screen-printing techniques with the same process as that for symmetric cell fabrication.

### 2.2. Characterization

Structural characterizations of YCFO, SDC and YCFO–SDC powders were carried out by powder X-ray diffraction (XRD) using a Philips X'pert PROS diffractometer with  $Cu-K_{\alpha}$  radiation at room temperature. The electrical conductivity measurement of YCFO pellets was conducted using a four-probe direct current (DC) technique. The impedance spectra of the symmetric cells were investigated using an Electrochemical Workstation (IM6e, Zahner). The measurements were conducted from 500 to 650 °C in a dry  $O_2$ – $N_2$  atmosphere over a frequency range from 0.1 Hz to 1 MHz

with a 10 mV AC signal amplitude. The oxygen partial pressures in  $O_2$ – $N_2$  atmosphere were controlled at  $0.01 \times 10^5$ ,  $0.10 \times 10^5$ ,  $0.21 \times 10^5$  and  $1.00 \times 10^5$  Pa using a mass flow controller.

Single cells were tested from 500 to 650 °C in a home-developed cell testing system with humidified ( $\sim 3\% H_2O$ )  $H_2$  and ambient air as reactant. The flow rate of hydrogen was  $40 \text{ ml min}^{-1}$ . The AC impedance spectra and discharging performance of single cells were measured using an electrochemical workstation (IM6e, Zahner). Fracture microstructure of tested cells was analyzed using a JEOL scanning electron microscopy (SEM, JXA-8100).

## 3. Results and discussion

### 3.1. XRD characterization

Fig. 1 shows the X-ray diffraction (XRD) pattern of  $Y_{2.5}Ca_{0.5}Fe_5O_{12-\delta}$  (YCFO) powders sintered at 1100 °C for 2 h. All observed diffraction peaks of the YCFO sample can be well indexed based on a cubic garnet structure (PDF #430507) with a simulated lattice parameter of 12.3511 Å. XRD patterns of SDC powders (as a reference) and YCFO–SDC mixture are also shown in Fig. 1(b) and (c), respectively. According to Fig. 1(c), those diffraction peaks of the YCFO–SDC powders can be referred clearly to either YCFO or SDC phase, indicating that the YCFO cathode will be chemically stable with the use of SDC electrolyte at the tested temperature.

### 3.2. Impedance spectra for symmetric cells

Fig. 2 shows the impedance spectra of the symmetrical cells using the YCFO–SDC $x$  ( $x = 0, 30, 40, 50, 60$ , the SDC weight percentage) composite cathodes measured at 650 °C in air. The determined polarization resistances ( $R_p$ ) are shown in Fig. 3 as functions of weight ratio of the SDC and the tested temperature. The polarization resistance firstly reduces with the increase of the SDC weight ratio, and it reaches a minimum at SDC of 40 wt.%. Actual  $R_p$  values are 9.99, 0.77, 0.55, 5.21 and 5.49  $\Omega\text{cm}^2$  at the SDC weight ratio of 0%, 30%, 40%, 50%, and 60%, respectively. This behavior is in fact consistent with the statement that the length of triple-phase boundaries could be greatly enlarged by introducing a suitable amount of ionic conducting phase into the composite cathode [3,7,29].

Linear temperature dependences of  $R_p$  for the YCFO-based composite electrodes are shown in Fig. 4. This linear dependence

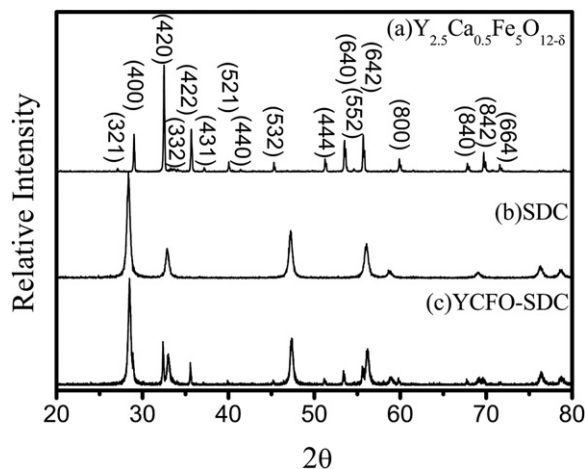


Fig. 1. X-ray diffraction patterns of  $Y_{2.5}Ca_{0.5}Fe_5O_{12-\delta}$  (YCFO),  $Ce_{0.8}Sm_{0.2}O_{1.9}$  (SDC) and YCFO–SDC powders. YCFO–SDC powders in the weight ratio of 1:1 were co-fired at 1100 °C for 2 h.

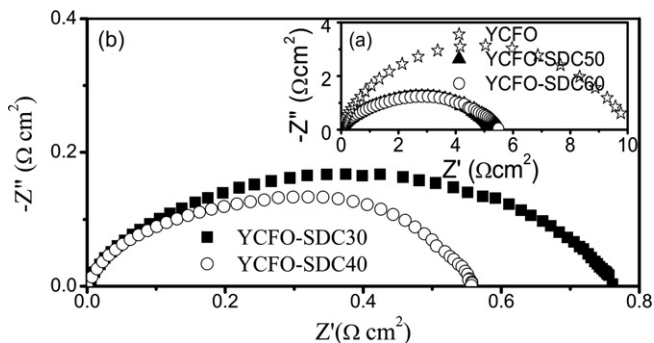


Fig. 2. Impedance spectra of the symmetric cells tested at 650 °C based on YCFO–SDC $x$  composite cathodes.

for every tested electrode in the studied temperature range implies the same reaction mechanism. For the YCFO single-phase electrode, the  $R_p$  values are 312.21, 81.30, 28.94 and 9.99  $\Omega\text{cm}^2$  measured at 500, 550, 600 and 650 °C, respectively. And for the YCFO–SDC40 composite electrode, they are 11.81, 3.48, 1.43, and 0.55  $\Omega\text{cm}^2$ , respectively. The activation energies for such YCFO-based electrodes are in the range of 1.38–1.22 eV. For comparison, the polarization resistances of  $\text{La}_{0.6}\text{Sr}_{0.4}\text{Co}_{0.2}\text{Fe}_{0.8}\text{O}_{3-\delta}$  (LSCF) [2] and  $\text{LSCF}-\text{Ce}_{0.8}\text{Gd}_{0.2}\text{O}_3$  (GDC) electrodes [2] are also shown in Fig. 4. The polarization resistance with the LSCF single-phase electrode is 1.10  $\Omega\text{cm}^2$  measured at 650 °C [2], approximately an order of magnitude smaller than that with the pure YCFO electrode, suggesting a much faster reaction rate when using the LSCF single-phase electrode. Fortunately, the polarization resistance of our new YCFO–SDC40 composite electrode is very close to that with LSCF–GDC (40 wt.%) (also shown in Fig. 4), especially at temperatures lower than 600 °C because of a smaller activation energy. The value of the polarization resistance of the LSCF–GDC composite electrode was 0.27  $\Omega\text{cm}^2$  at 650 °C [2].

Fig. 5 shows the temperature dependence of electrical conductivity of the YCFO sample in air measured by the four-probe method. Conductivity of the YCFO sample increases when increasing the temperature. It is approximately 0.69, 0.87 and 1.01  $\text{Scm}^{-1}$  measured at 500, 600 and 700 °C, respectively. Conductivity of the YCFO sample is approximately 2–3 orders of magnitude lower than that of LSCF ( $>300 \text{Scm}^{-1}$  at 750 °C [2]) and SSC ( $\sim 10^3 \text{Scm}^{-1}$  [9]), which might be the reason to explain the

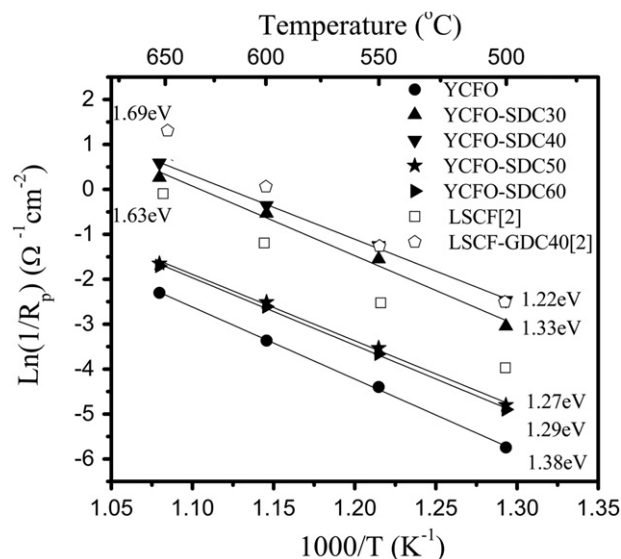


Fig. 4. Temperature dependences of the interfacial polarization resistances ( $R_p$ ) using YCFO–SDC $x$  cathodes,  $\text{La}_{0.6}\text{Sr}_{0.4}\text{Co}_{0.2}\text{Fe}_{0.8}\text{O}_{3-\delta}$  (LSCF) cathode [2], and  $\text{LSCF}-\text{Ce}_{0.8}\text{Gd}_{0.2}\text{O}_3$  (GDC) cathode [2].

observed large polarization resistance with the YCFO single-phase electrode. The lowered polarization resistances of the YCFO–SDC40 composite cathode may also imply that the enlarged length of triple-phase boundaries might have a larger beneficial effect on the cathode behavior than the intrinsic electrical conductivity of the used electrode materials.

Dependence of polarization resistance on oxygen partial pressure was investigated in order to clarify the possible rate-limiting steps for the YCFO-based composite electrodes. Fig. 6 shows typical impedance spectra of the YCFO–SDC40 composite electrode measured at various oxygen partial pressures at 650 °C. Two depressed semicircles could be clearly observed in these spectra, indicating at least two limiting reaction steps for the oxygen reduction reaction. The length of low frequency arc reduces much faster with the increase of oxygen partial pressure than that of the high frequency arc does. An equivalent circuit composed of two RQ

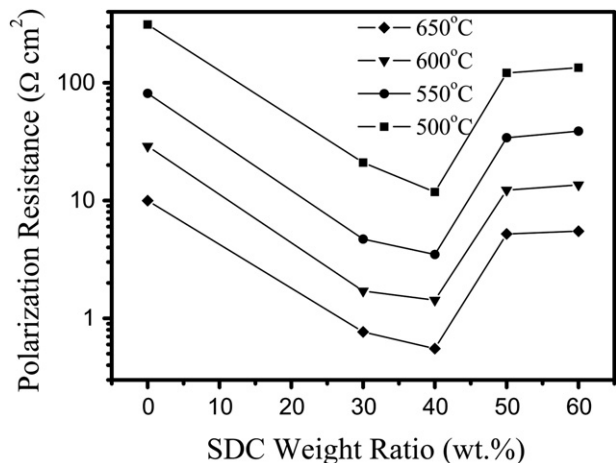


Fig. 3. Polarization resistances ( $R_p$ ) of the symmetric cells as a function of the SDC weight ratio in the YCFO–SDC composite cathodes.

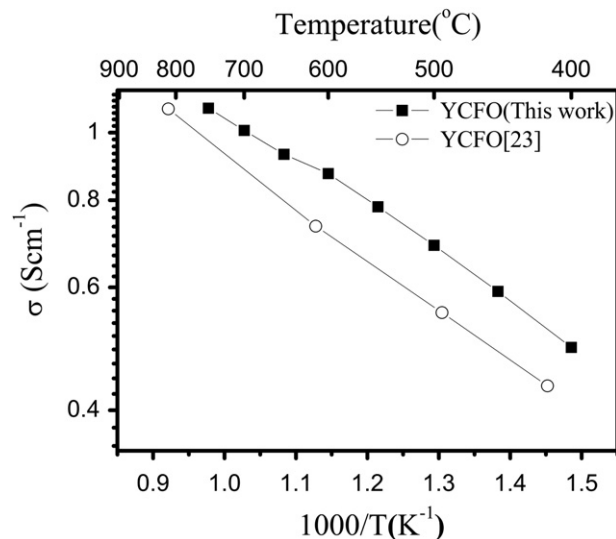


Fig. 5. Electrical conductivity of the  $\text{Y}_{2.5}\text{Ca}_{0.5}\text{Fe}_5\text{O}_{12}$  samples sintered at 1350 °C for 5 h measured in air.

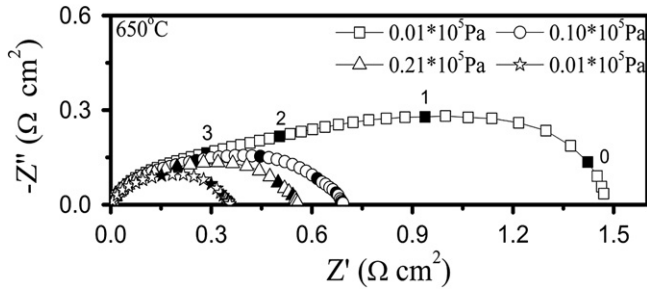


Fig. 6. Impedance spectra of the symmetric cell with YCF0-SDC40 composite electrode measured in dry N<sub>2</sub>-O<sub>2</sub> atmosphere with various oxygen partial pressures.

elements ( $R_H Q_H$ ) ( $R_L Q_L$ ) is proposed to resolve these spectra, where  $R$  represents the polarization resistance,  $Q$  represents the constant-phase element, and the subscripts H and L correspond to the high and low frequency arc, respectively. The dependence of  $R_H$  and  $R_L$  on oxygen partial pressure ( $P_{O_2}$ ) can be presented in a common format,  $R_i \propto P_{O_2}^{-m}$ , where  $m$  is the reaction order of  $R_i$  with respect to  $P_{O_2}$ . As shown in Fig. 7,  $R_H$  is almost independent of  $P_{O_2}$  with a reaction order of 0.07 (error of 3.5%), indicating an oxygen ion diffusion rate-limiting step [18]. The reaction order of  $R_L$  is 0.63 (error of 1.9%), which is intermediate between 0.5 and 1.0, indicating both a dissociative adsorption-limiting step (for  $m = 0.5$ ) and a gas-phase diffusion-limiting step (for  $m = 1$ ) [30]. Improved electrochemical reaction rate could thus be highly anticipated with the optimization of electrode microstructure because of its beneficial effect on gas-phase diffusion-limiting step. At  $0.21 \times 10^5$  Pa and 650 °C, the simulated  $R_H$  and  $R_L$  are 0.37 and 0.18  $\Omega\text{cm}^2$  with the capacitances of  $2.10 \times 10^{-4} \text{ Fcm}^{-2}$  and  $5.76 \times 10^{-3} \text{ Fcm}^{-2}$ , respectively.

### 3.3. Performance of single cells

Fig. 8 shows the cross-sectional view of a tested single cell with YCF0-SDC40 composite cathode. The cathode adheres well to the SDC electrolyte, and no reaction layer is observed between the electrolyte and the cathode. The thickness of the cathode and the electrolyte film are approximately 50 and 40  $\mu\text{m}$ , respectively.

Fig. 9 shows the impedance spectra of the single cells with YCF0-SDC40 cathode. The total resistances of the cells are 1.95,

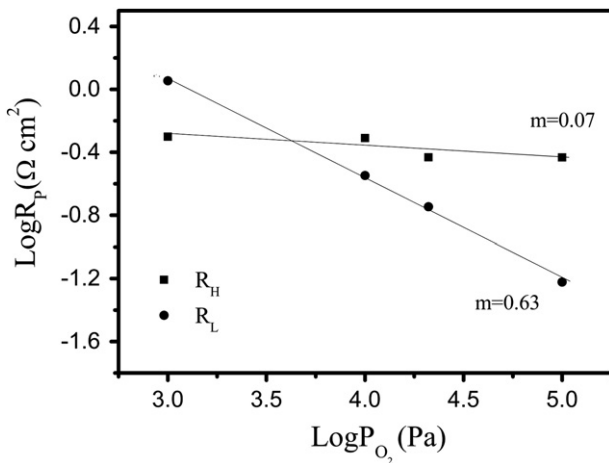


Fig. 7. The simulated high frequency polarization resistance ( $R_H$ ) and low frequency polarization resistance ( $R_L$ ) of the cell with the YCF0-SDC40 composite electrode as a function of oxygen partial pressures in dry N<sub>2</sub>-O<sub>2</sub> atmospheres.

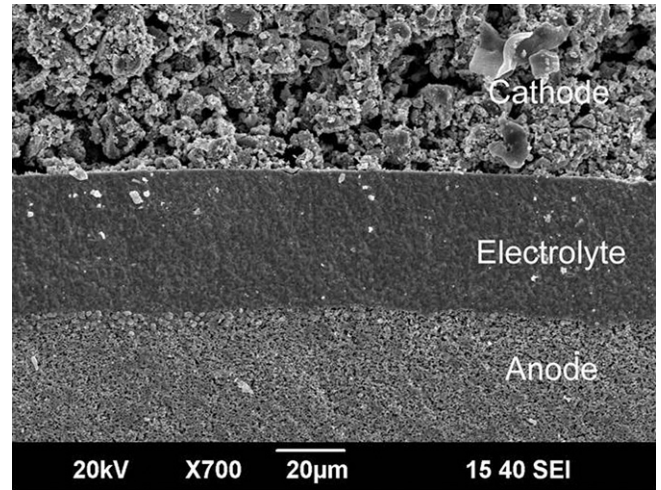


Fig. 8. SEM image of the cross-section of a tested single cell.

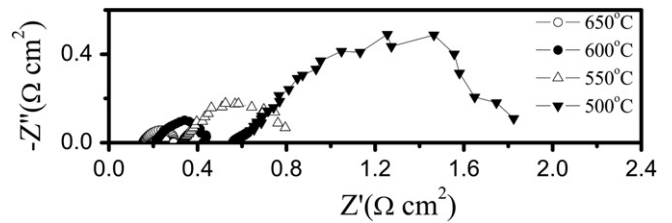


Fig. 9. Impedance spectra of a single cell with YCF0-SDC40 composite cathode measured at various temperatures.

0.86, 0.46 and 0.29  $\Omega\text{cm}^2$  at 500, 550, 600 and 650 °C, respectively. The polarization resistances of the cells are 1.38, 0.54, 0.25, and 0.14  $\Omega\text{cm}^2$  at 500, 550, 600, and 650 °C, respectively, which are much lower than that of the above symmetric cells. This might result from the partial electronic conductivity of the SDC electrolyte at the operating atmosphere, which activates the electrode reaction. Fig. 10 shows the  $I-V$  and  $I-P$  curves of the single cell with YCF0-SDC40 composite cathode measured from 500 to 650 °C. The maximum power densities with the values of 113, 221, 351, and 438  $\text{mW cm}^{-2}$  are obtained at 500, 550, 600, and 650 °C, respectively. The values of these maximum power output are very close

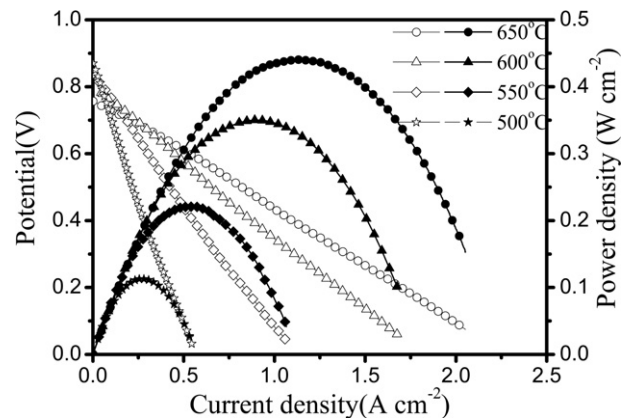


Fig. 10.  $I-V$  and  $I-P$  curves of the single cell with the YCF0-SDC40 composite cathode measured at various temperatures.

to those with LSCF ( $350 \text{ mW cm}^{-2}$  at  $700 \text{ }^\circ\text{C}$  [2]) and SSC ( $350\text{--}400 \text{ mW cm}^{-2}$  at  $600 \text{ }^\circ\text{C}$  [8,11]) based composite cathodes, suggesting that the YCFO-based composite electrode could become an alternative, low-cost but electrochemically active cathode for future IT-SOFCs.

#### 4. Conclusions

An iron garnet,  $\text{Y}_{2.5}\text{Ca}_{0.5}\text{Fe}_5\text{O}_{12-\delta}$  (YCFO), was fully characterized as a promising cathode material for intermediate temperature solid oxide fuel cells. The polarization resistance with YCFO single-phase cathode was  $9.99 \text{ } \Omega\text{cm}^2$  at  $650 \text{ }^\circ\text{C}$ , about an order of magnitude larger than that with  $\text{La}_{0.6}\text{Sr}_{0.4}\text{Co}_{0.2}\text{Fe}_{0.8}\text{O}_{3-\delta}$  single-phase cathode. The conductivity measurements suggested that the low conductivity of YCFO should account for the large polarization resistance of the YCFO single-phase cathode. With the introduction of  $\text{Ce}_{0.8}\text{Sm}_{0.2}\text{O}_{1.9}$  ionic conducting phase to enlarge the length of triple-phase boundaries, the polarization resistances of YCFO-based composite cathodes reduced greatly and reached a minimum at SDC of 40 wt.%. The low polarization resistance value of the YCFO–SDC40 cathode, approximately  $0.55 \text{ } \Omega\text{cm}^2$  at  $650 \text{ }^\circ\text{C}$ , is close to that with LSCF–GDC (40 wt.%) composite cathode, implying that the introduction of an ionic conducting phase has a more important effect on the reaction rate than the conductivity of the material. With YCFO–SDC40 as composite cathode, the maximum power density of the cell was  $438 \text{ mW cm}^{-2}$  measured at  $650 \text{ }^\circ\text{C}$ . Such electro-performances of the cells indicate that the YCFO-based composite materials could become a promising and low-cost cathode for future IT-SOFCs.

#### Acknowledgements

This work was financially supported by the Natural Science Foundation of China (51072193), National Basic Research Program of China (973 Program, 2012CB922001), and the Fundamental Research Funds for the Central Universities.

#### References

- [1] S.Y. Wang, J. Yoon, G. Kim, D.X. Huang, H.Y. Wang, A.J. Jacobson, *Chem. Mater.* 22 (2009) 776–782.
- [2] E. Perry Murray, M.J. Sever, S.A. Barnett, *Solid State Ionics* 148 (2002) 27–34.
- [3] V. Dusastre, J.A. Kilner, *Solid State Ionics* 126 (1999) 163–174.
- [4] N. Oishi, A. Atkinson, N.P. Brandon, J.A. Kilner, B.C.H. Steele, *J. Am. Ceram. Soc.* 88 (2005) 1394–1396.
- [5] J.M. Bae, B.C.H. Steele, *Solid State Ionics* 106 (1998) 247–253.
- [6] H.Y. Tu, Y. Takeda, N. Imanishi, O. Yamamoto, *Solid State Ionics* 117 (1999) 277–281.
- [7] C.R. Xia, W. Rauch, F.L. Chen, M.L. Liu, *Solid State Ionics* 149 (2002) 11–19.
- [8] C.R. Xia, M.L. Liu, *Solid State Ionics* 144 (2001) 249–255.
- [9] H. Fukunaga, M. Koyama, N. Takahashi, C. Wen, K. Yamada, *Solid State Ionics* 132 (2000) 279–285.
- [10] S.Z. Wang, H. Zhong, *J. Power Sources* 165 (2007) 58–64.
- [11] Z.P. Shao, S.M. Haile, *Nature* 431 (2004) 170–173.
- [12] K. Wang, R. Ran, W. Zhou, H.X. Gu, Z.P. Shao, J. Ahn, *J. Power Sources* 179 (2008) 60–68.
- [13] Z.H. Chen, R. Ran, W. Zhou, Z.P. Shao, S.M. Liu, *Electrochim. Acta* 52 (2007) 7343–7351.
- [14] Z.P. Shao, S.M. Haile, J. Ahn, P.D. Ronney, Z.L. Zhan, S.A. Barnett, *Nature* 435 (2005) 795–798.
- [15] C. Frontera, A. Caneiro, A.E. Carrillo, J. Oró-Solé, J.L. García-Muñoz, *Chem. Mater.* 17 (2005) 5439–5445.
- [16] V. Pralong, V. Caignaert, S. Hebert, A. Maignan, B. Raveau, *Solid State Ionics* 177 (2006) 1879–1881.
- [17] H.T. Gu, H. Chen, L. Gao, Y.F. Zheng, X.F. Zhu, L.C. Guo, *Int. J. Hydrogen Energy* 34 (2009) 2416–2420.
- [18] D.J. Chen, R. Ran, K. Zhang, J. Wang, Z.P. Shao, *J. Power Sources* 188 (2009) 96–105.
- [19] J. Wan, J.B. Goodenough, J.H. Zhu, *Solid State Ionics* 178 (2007) 281–286.
- [20] A. Aguadero, J.A. Alonso, M.J. Escudero, L. Daza, *Solid State Ionics* 179 (2008) 393–400.
- [21] B. Wei, Z. Lü, X.Q. Huang, M.L. Liu, N. Li, W.H. Su, *J. Power Sources* 176 (2008) 1–8.
- [22] C. Milanese, V. Buscaglia, F. Maglia, U. Anselmi-Tamburini, *Chem. Mater.* 16 (2004) 1232–1239.
- [23] V.V. Kharton, A.L. Shaula, E.N. Naumovich, N.P. Vyshatko, I.P. Marozau, A.P. Viskup, F.M.B. Marques, *J. Electrochem. Soc.* 150 (2003) J33–J42.
- [24] H.C. Yu, K.Z. Fung, *J. Power Sources* 133 (2004) 162–168.
- [25] S. Sameshima, T. Ichikawa, M. Kawaminami, Y. Hirata, *Mater. Chem. Phys.* 61 (1999) 31–35.
- [26] H. Runge, U. Guth, *J. Solid State Electrochem.* 8 (2004) 272–276.
- [27] R.R. Peng, C.R. Xia, Q.X. Fu, G.Y. Meng, D.K. Peng, *Mater. Lett.* 56 (2002) 1043–1047.
- [28] F. Zhao, Z.Y. Wang, M.F. Liu, L. Zhang, C.R. Xia, F.L. Chen, *J. Power Sources* 185 (2008) 13–18.
- [29] E. Perry Murray, S.A. Barnett, *Solid State Ionics* 143 (2001) 265–273.
- [30] A. Ringuedé, J. Fouletier, *Solid State Ionics* 139 (2001) 167–177.